Available online at www.sciencedirect.com

ScienceDirect

Procedia CIRP 109 (2022) 562–567

www.elsevier.com/locate/procedia

32nd CIRP Design Conference

Approach to optimize the interlayer waiting time in additive manufacturing with concrete utilizing FEM modeling

Virama Ekanayaka[a]*, Lukas Lachmayer[b], Annika Raatz[b], André Hürkamp[a]

[a]*Technische Univeristät Braunschweig, Institute of Machine Tools and Production Technology, Langer Kamp 19b, 38106 Braunschweig, Germany*
[b]*Leibniz Universität Hannover, Institute of Assembly Technology, An der Universität 2, 30823 Garbsen, Germany*

* Corresponding author. Tel.: +49 (0)531 / 391 - 7668 , E-*mail address:* v.ekanayaka@tu-braunschweig.de

Abstract

Additive manufacturing processes show potential and utility in the construction industry by enabling new design freedoms and increasing the degree of automation. Accurate prediction of structural deformations and optimization of process parameters is a crucial consideration to ensure better component quality, reduced test effort and fewer buildability failures. This paper introduces an approach to build a nonlinear model that maps the interlayer waiting time in the building process to the corresponding structural deformation based on FEM results obtained from a process based FEM simulation. The model is utilized to optimize the interlayer waiting time during the printing process using the maximum deformation of the structure as the objective function and the allocated printing time together with the allowed maximum interlayer waiting time as constraints. Finally, the validity of the approach is numerically verified using a test component.

Keywords: process optimization; finite element modeling; constrained optimization; additive manufacturing in construction; concrete printing

1. Introduction

The construction industry is currently facing two significant challenges. On the one hand, there is a considerable shortage of well-trained specialists, particularly in high-wage countries. On the other hand, more environmentally friendly construction processes must be created to consume fewer resources and use them more efficiently in terms of sustainability [1].

In this sense, additive manufacturing processes offer enormous potential for overcoming future challenges [2]. Such processes are characterized by high automation, requiring fewer skilled personnel and offering more component design freedom than conventional processes. While the first aspect can solve the staff issues, the latter opens the possibility of using less material in a more force-flow-oriented manner, thus reducing the overall resource requirements.

One of the most significant material saving potential in the construction industry is attributed to the elimination of formwork components. Particularly for complex geometries, specific single-use solutions are designed to keep the fresh concrete in place. Since no reuse is possible, these structures are then disposed and thus account for a significant proportion of waste generation [3].

However, the widespread introduction of additive manufacturing processes to avoid such one-off formwork is currently confronted with the time-dependent material behavior of fresh concrete. An important consideration when manufacturing components with concrete is the considerably longer curing time as compared to plastics or other conventional material. While curing accelerator essentially

10.1016/j.procir.2022.05.295

reduces the period, the rheology of the material is still measurable up to several minutes [4]. This makes it necessary to explicitly consider the time-dependent flow behavior of the material for the additive manufacturing of the designed concrete components. If not, the rheology can result in printing failure by elastic buckling or plastic collapse.

Therefore, the buildability of a material is used as a measurement to predict a potential printing collapse. It is defined as the number of printable layers without elastic or plastic collapse of previously printed parts [5]. For the individual layers, the layer geometry (layer width and layer height) are determined by the deposition rate, nozzle velocity and nozzle distance to the printing surface [6]. For single experiments, it is sufficient to determine the buildability with small-scale experiments and use the results for an estimation [7, 8]. However, the long-term implementation of additive manufacturing approaches in the construction sector requires a more systematic and general approach. Therefore, a model-based description of the printing process can be combined with a representation of the time-dependent material properties to simulate the component deformation during the printing process [9, 10, 11, 12].

This paper presents an advanced method to enhance the process-based simulation using the finite element method (FEM). This methodology can be utilized to predict and minimize deformations of the designed part. In the presented approach, the interlayer waiting time is optimized to reduce the risk of printing failure and increase the accuracy of the designed part while keeping up the interlayer strength and realize a dedicated printing time. The validity of the presented approach is numerically verified using a test component.

2. Deformation prediction and minimization in additive manufacturing processes

2.1. Finite element analysis in additive manufacturing

The prediction of deformation and residual stress of a structure is crucial in determining its structural properties. This is especially true when it comes to 3D printing with concrete which requires accurate deformation predictions and precise process settings due to its time dependent rheological properties to ensure that the manufactured part lies within the tolerances specified in the design. Furthermore, the precision of the process settings ensure that manufacturing constraints such as the total time of printing are not violated. Finite element analysis (FEA) of extrusion-based additive manufacturing processes of concrete highlights the complex interactions between process and material parameters [13].

In a standard structural FEA the deformations and stresses of a fixed input geometry are calculated, whereas in AM simulations the input geometry itself is changing with time as new layers are added on top of the existing layers, which adds an additional layer of complexity to the simulated model. Current commercial FEA software is capable of handling simulations of structures manufactured using various AM technologies [14, 15, 16].

The general procedure for carrying out standard FEM simulations using commercial software is similar, where the target CAD geometry is initially uploaded with the corresponding boundary conditions, material properties and external forces. The structure is then meshed and the governing physical equations are discretized and solved to obtain nodal displacements. Secondary variables such as strain and stress can be subsequently determined.

For the simulation of the 3D printing process a numerical interpretation is required by the FEA-software which mimics the material deposition. This is achieved via an automated element activation which translates to an event series inputs in time and space. Commercial software such as ABAQUS contain an event series module which is utilized to prescribe the imposed tool path and process parameter such as the printing speed and material deposition thickness [17]. Once the 3D printing process is translated into the event series format, the mesh intersection with the tool path automatically computes the relevant information required for the FEA such as the active elements, corresponding material properties, external forces and boundary conditions for each given time step [17].

An alternate approach has been developed where the G-Code containing the printing information required by the 3D printer such as the toolpath, feed rate, etc. is utilized to create the FEM model in additive manufacturing. For the simulation, the target CAD geometry is used and data from the G-Code is decoded to determine the active elements in the mesh [18].

The limitation of such approaches is that the target CAD geometry is used for the analysis. However, depending on the printing path, the printed geometry would have deviations from the target geometry even before deformation due to stress are considered. To overcome this limitation and achieve a more detailed modelling of the AM process, an FEM model constructed directly from the printing path has been presented in an earlier publication by Lachmayer et al. [19]. This modeling approach is briefly summarized in section 3 and will be used to generate the simulation results required to build the nonlinear model and the subsequent optimization.

2.2. Current approaches to minimize component deformations during printing

With the recent rise in popularity of 3D printing, a lot of research has gone into minimizing structural deformation to ensure as close a match to the target geometry as possible. Issues such as warpage, shrinkage, curling, etc. that results from temperature gradients and other printing effects are being adequately investigated [20, 21, 22].

The research into the minimization of structural deviation during the manufacturing process is even more significant in the construction industry since much larger components are manufactured. For concrete, the time dependent behavior of the admixture plays a crucial role in the deformations of the structure [23, 24]. The rheology of 3D printed concrete structures depend strongly on the material properties, which in turn depends on the elapsed time. Additional time for material hardening can be enabled by allowing an interlayer waiting time between the layers. In this context, an interlayer waiting time refers to a pause in the printing process before additional layers are printed onto the top layer of the existing structure.

An additional consideration that needs to be made when allowing for interlayer waiting time is that this could negatively affect the mechanical interlocking between strands which leads to reduced component strength [4]. A further option is the addition of accelerator to the concrete mixture to expedite its hardening. A significant increase in yield stress after deposition and in yield stress evolution over time is observed when adding accelerator, which enables a higher vertical building rate, making it highly relevant for practical applications [4].

The maximum vertical deviation between as designed and as manufactured of the structure occurs as expected on the topmost layer since all the deformations of the underlying layers are accumulated. The crucial point to be noticed when considering such structural deformations is that no linear relationship between the maximum deviation and the number of underlying layers exists, since underlying layers exhibit varying degrees of plastic deformation. Allowing an interlayer waiting time reduces the maximum deviation of the structure, but this time cannot be arbitrarily long because the maximum total time available (printing time plus interlayer waiting time) could be constrained by parallel component production as well as the natural constraint of reduced mechanical interlocking with increasing interlayer waiting time [4]. This presents an optimization opportunity, which to the best of the authors' knowledge has not been addressed yet. In this paper, this problem will be formulated as a constrained optimization task and solved using the Lagrange multiplier method.

3. Process based finite element analysis

In this section, a brief summary of generating the mesh geometry and the subsequent FEM simulation is provided [19]. The material applied from the nozzle at a waypoint $\bar{p}_i$ is modelled as a circular patch with radius r_i. The mesh geometry can then be constructed using the waypoint coordinates and the path thickness, as illustrated in Fig 1, where *ds* defines the size of a single element.

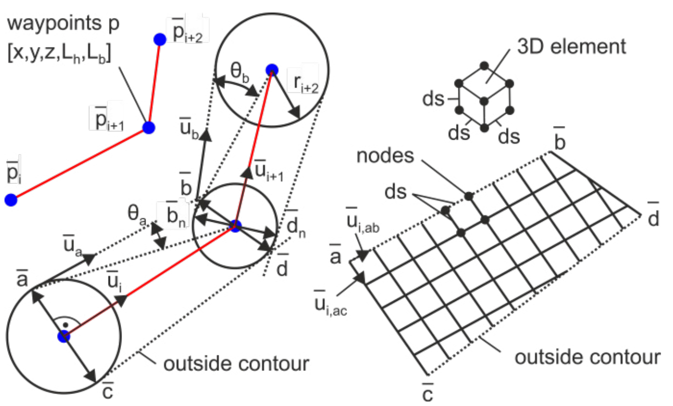

Fig. 1. Waypoint to FEM mesh conversion [19]

In the initial step a two dimensional quadrilateral is formed between two successive path points. The quadrilateral will then be meshed in 2D as shown in the above figure 1 and the 3D mesh is created by repeatedly shifting the 2D nodes along the z-direction by *ds* until the specified layer height is reached.

The geometry of the quadrilateral is specified by the points $\bar{a}$, $\bar{b}$, $\bar{c}$ and $\bar{d}$, whose coordinates are primarily determined by the two unit vectors $\bar{u}_i$ and $\bar{u}_{i+1}$. Each element in the mesh gets an individual time stamp derived from its position and nozzle velocity. Since the material properties of concrete change during the printing process, the time stamp will be utilized in the simulation to determine the current material value based on the elapsed time. To incorporate the interlayer waiting time, the individual time stamps of all elements in the layer are increased by the corresponding interlayer waiting time. The entire code has been implemented in MATLAB and the data flow of the simulation process is summarized in Fig 2.

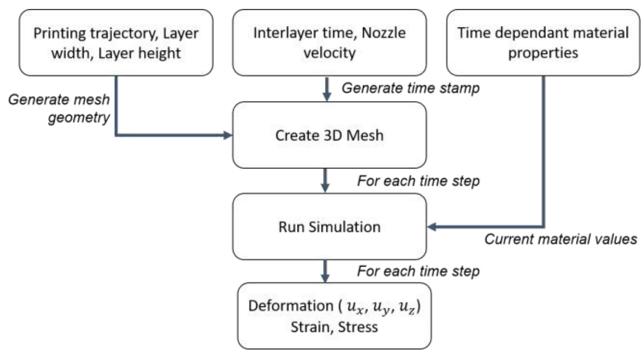

Fig. 2. Simulation data flow

The printing trajectory and printing parameters are required to construct the geometry of the printed structure and the interlayer time along with the nozzle velocity is used to determine the time stamp of the element. The time stamp of the element is utilized to calculate the actual values of the material properties, which directly determines the deformation. The complete derivation of the equations used to construct the geometry were presented in a previous publication [19]. An implicit analysis was used for the FEA simulation. In order to use the response surface methodology described in section 4 a dataset of simulation results is created. A five layer curved wall section as displayed in Fig 3 is simulated with varying interlayer waiting times and the resulting z-deformation of the nodes are stored.

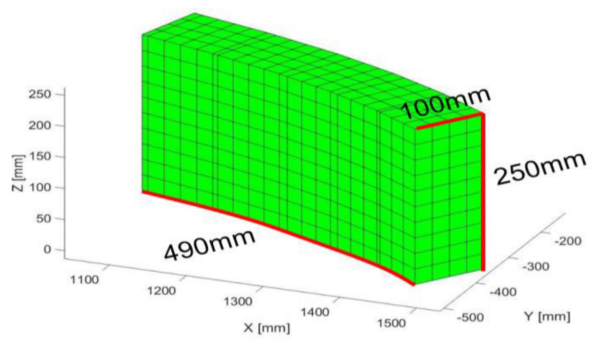

Fig. 3. Dimension of curved wall section

This is a resupply of March 2023 as the template used in the publication of the original article contained errors. The content of the article has remained unaffected.

4. Response surface method and the constrained optimization task

The response surface methodology can be used to construct a nonlinear function that maps the interlayer waiting time into the maximum z-deformation. The interlayer waiting time of the FEM Model constitutes the input and the maximum nodal deviation obtained from the simulation is the corresponding output. The input space equals the number of interlayers, but for the purpose of visualization a 2D input space is shown is Fig 4. It should be noted that this figure was constructed to illustrate the optimization concept using the response surface methodology. It does not correspond to the actual deformation of the parametric study.

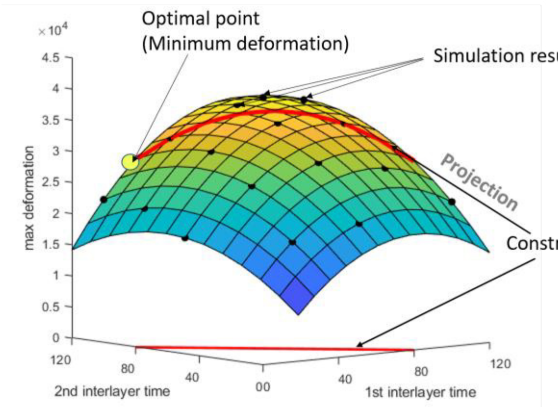

Fig. 4. Constrained optimization using the response surface method

The points shown in black are the results obtained from the simulations. Then a surface described by a nonlinear equation

$$f(t_1, t_2) = \beta_0 + \beta_1 \cdot t_1 + \beta_2 \cdot t_2 + \beta_3 \cdot {t_1}^2 + \beta_4 \cdot {t_2}^2 \quad (1)$$

can be fitted onto the simulation data points. The coefficients β_0 to β_4 are determined through non-linear least squares regression. When fitting a function into a larger input space more coefficients have to be determined which requires more data points for an accurate fitting. The optimization task is to find the combination of interlayer waiting times which result in the minimum deviation of the structure. This optimization is carried out under the constraint that the total interlayer waiting time should not exceed a fixed value, to ensure a fixed printing time for a component. The constraint can be formulated as

$$\sum_i t_i = t_{tot} = constant \quad (2)$$

and is indicated by the red line in Fig 4. Here t_i is the interlayer waiting time for layer i and t_{tot} is the sum of the interlayer waiting times. This constraint is projected onto the output and the minimum deviation point (indicated in yellow) on the projected line is the point that needs to be determined. For a higher input space the constraint will be a projection in hyperspace where additional inequality constraints can be imposed. When determining the optimal distribution of the interlayer waiting time, it should be enforced that no single interlayer waiting time should exceed a time t_{max} after which the component strength deteriorates due to reduced mechanical interlocking between the layers. Once the nonlinear function $f(t_i)$is obtained, the constrained optimization can be carried out using the Lagrange multiplier method.
It should be noted that the optimization is purely carried out on the interlayer waiting times. All other printing parameters such as the nozzle velocity, concrete admixture and total printing time are kept constant.

5. Numerical verification of the approach with a test component

To verify the proposed approach a test component of a curved wall consisting of five layers with individual layer height of 50 mm was simulated with varying time intervals between the layers. The 5 layers correspond to 4 interlayer waiting times t_1 to t_4. The maximum value t_{max} allowed for each individual interlayer waiting time is 2 minutes. To ensure a fixed component production time the total sum of the interlayer waiting times was constrained to be 4 minutes. The material parameters used for the simulation can be seen in table 1, where t is in seconds.

Material parameters	
Density $[kN/m^3]$	2060
Elasticity modulus $[MPa]$	$0.078 + 0.00002t$
Poisson ratio	0.3
Cohesion	$3.05 + 0.058t$

Table 1. Material properties used for the simulation

The density, Poisson ratio and cohesion values for 3D printing concrete are taken from [25]. The given elastic modulus function can be achieved by the addition of accelerator to the admixture [4].

The full factorial method used in the design of experiments was utilized to generate the input data set for the simulations. Five levels were chosen for each of the four interlayer waiting times $t_i = \{0, 30, 60, 90, 120\}$.This produces a total of 625 (5^4) simulations, which were carried out with the varying combinations of the interlayer waiting times and the maximum deviation in the vertical z-direction was recorded. The generated data was fitted by the following nonlinear model.

$$f(t_i) = \beta_0 + \sum_{i=1}^{4} \beta_{2i-1} \cdot {t_i}^{\beta_{2i}} \quad (3)$$

The nine coefficients of the model which were determined through nonlinear regression are shown in table 2.

β_0	β_1	β_2	β_3	β_4	β_5	β_6	β_7	β_8
8.3597	-0.0080	0.8599	-0.0127	0.8588	-0.0139	0.8031	0.0126	0.7833

Table 2. Coefficient values of nonlinear model

The model shows a coefficient of determination - R^2 of 0.994, which translates to an accuracy of 99.4% in fitting the simulation data. The $p - value$ is 0 which indicates that there exists a very strong correlation between the interlayer waiting time and the deformation of the structure.

For the generated dataset the minimum deviation was obtained as expected for the largest interlayer waiting time distribution $\{120,120,120,120\} = 6.0306mm$ and the maximum deviation for the smallest interlayer waiting times $\{0,0,0,0\} = 8.5326mm$. The minimum deviation for the data set under the given constraint that $t_{max} \leq 240s$ was for the interlayer waiting time distribution$\{0,120,90,30\} = 6.8569mm$.

In the subsequent step the arguments t_i of the objective function (3) which result in the minimum deformation under the given constrains were determined by the Lagrange multiplier method to be as follows.

t_1	t_2	t_3	t_4
20.9147	120	69.4837	20.6016

Table 3. Values for optimal interlayer waiting times

The fact that the actual optimum lies on the constraint $t_{max} = 240s$ is to be expected, since the greater the total interlayer waiting time, the smaller is the final deformation.

Finally, simulations were carried out with the optimal interlayer waiting times and three additional combinations for comparison. The three additional combinations were chosen to analyse how the predicted optimal distribution of interlayer waiting times compare with a uniform distribution and with interlayer waiting times concentrated at the top and bottom of the structure. The results are shown in Fig 5.

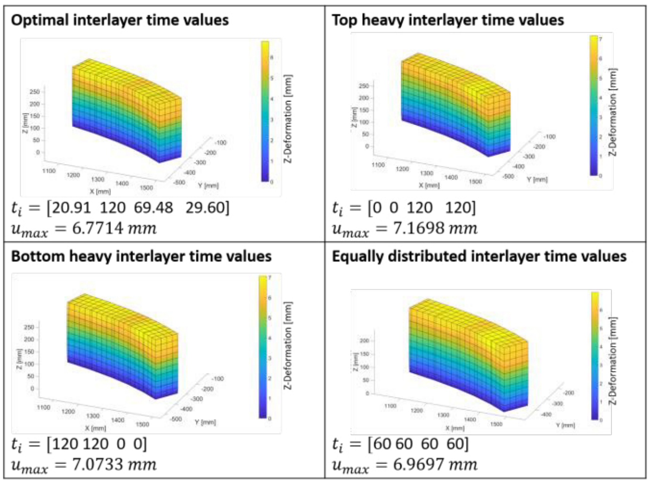

Fig. 5. FEM simulation results

The results indicate that an optimal distribution of the interlayer waiting time values exist when minimizing the component deformation. Since in the optimal value distribution the largest values for the interlayer waiting time is allocated to the middle layers, it can be interpreted that a higher stiffness in the middle of the structure is more significant for the minimization of the deformation than at the top or bottom. This is completely plausible since the greatest weight is carried by the bottommost layers even though they have the longest time to harden. In contrast, since the topmost layers carry significantly less weight they require relatively less hardening time. Therefore, the critical region of the component is comprised of the middle layers.

6. Summary and outlook

Additive manufacturing processes currently indicate a good potential for its application in the construction industry. To ensure better component quality and mechanical strength as well as in enforcing design tolerances the process parameters have to be accurately determined. FEA play a key role to predetermine the discrepancy between the manufactured component and the original design and the subsequent optimization of the process parameters is essential to minimize component defects, deviations and to ensure the printed component lies within the allocated tolerances specified in the design.

This paper utilizes process based FEM simulation results to build a nonlinear model that maps interlayer waiting time during printing to the final deformation of the printed structure. The nonlinear model which is considered as the objective function was then optimized under given constraints to determine the optimal interlayer waiting times. The approach was numerically verified by means of a test component, which was a curved wall of 250 mm in height. It could be established that an optimal distribution of the interlayer waiting times exists and the results indicates that the structural strength of the middle of the component was more crucial to minimize the deformations as compared to the top or bottom. The limitation of the FEA model used in the optimization is that it does not capture the rheology of concrete optimally. The FEA model can be improved by utilizing a more sophisticated viscoelastic model to better capture the yield behaviour of fresh concrete and this will be even more relevant when considering larger components.

In future work this methodology can be applied to larger and more complex components in order to compare if the trend identified in this paper holds. Additionally the influence of other process parameters such as the individual layer height on the structural deformation can be investigated by the proposed approach.

Acknowledgements

The authors gratefully acknowledge the funding by the Deutsche Forschungsgemeinschaft (DFG – German Research Foundation) – Project no. 414265976. The authors would like to thank the DFG for the support within the SFB/Transregio 277 – Additive manufacturing in construction. (Subproject B04)

References

[1] Bos FP, Wolfs RJM, Amed ZY, Salet TAM. Additive manufacturing of concrete in construction: potentials and challenges of 3D concrete printing. Virtual and Physical Prototyping; 2016, 11, p. 209-225

[2] Paul SC, Zijl GPAG, Tan MJ, Gibson I. A review of 3D concrete printing systems and materials properties: current status and future research prospects. Rapid Prototyping Journal; 2018, 24, p. 784-798

[3] Tay YWD, Qian Y, Tan MJ. Printability region for 3D concrete printing using slump and slump flow test. Composites Part B; 2019, 174:1359-8368

[4] Dressler I, Freund N, Lowke D. The Effect of Accelerator Dosage on Fresh Concrete and on Interlayer Strength in Shotcrete 3D Printing. Materials; 2020, 13:2-374

[5] Nerella VB, Krause M, Mechtcherine V. Direct printing test for buildability of 3D-printable concrete considering economic viability. Automation in Construction; 2020, 109:0926-5805

[6] Ibrahim S, Olbrich A, Lindemann H, Gerbers R, Kloft H, Dröder K, Raatz A. Automated Additive Manufacturing of Concrete Structures without Formwork - Concept for Path Planning. Tagungsband des 3. Kongresses Montage Handhabung Industrieroboter 2018.

[7] Le TT, Austin SA, Lim S, Buswell RA, Gibb AGF, Thorpe T. Mix design and fresh properties for high-performance printing concrete. Materials and Structures; 2012, 45, p. 1221-1232

[8] Kazemian A, Yuan X, Cochran E, Khoshnevis B. Cementitious material for construction-scale 3D printing: Laboratory testing of fresh printing mixture. Construction and Building Materials; 2018, 145, p. 639-647

[9] Wolfs RJM, Bos FP, Salet TAM. Triaxial compression testing on early age concrete for numerical analysis of 3D concrete printing. Cement and Concrete Composites; 2019, 104:0958-9465

[10] Perrot A, Rangeard D, Pierre A. Structural built-up of cement-based materials used for 3D printing extrusion techniques. Materials and Structures; 2013, 49:1213-1220

[11] Camminal R, Silva WRL, Andersen TJ, Stang H, Spangenber J. Modelling of 3D concrete printing based on computational fluid dynamics. Cement and Concrete Research; 2020, 138:0008-8846

[12] Wolfs RJM, Bos FP, Salet TAM. Early age mechanical behaviour of 3D printed concrete: Numerical modelling and experimental test. Cement and Concrete Research; 2018, 106, p. 103-116

[13] Reinold J, Nerella VN, Mechtcherine V, Meschke G. Particle finite element simulation of extrusion processes of fresh concrete during 3d-concrete-printing. International Conference on Simulation for Additive Manufacturing, 2019

[14] Sagar KG, Suresh PM. 3D FEM analysis of extrusion process of al2024-Beryl composites. World Journal of Engineering Research and Technology, 2018

[15] Pagac M, Hajnys J, Halama R, Aldabash T, Mesicek J, Jancar L, Jansa J. Prediction of Model Distortion by in 3D Printing via the Selective Laser Melting of Stainless Steel AISI 316L. Applied sciences, 2021.

[16] Lee YT, Zhuang JR, Hsieh WH, Yang AS. FEM Simulations to Study the Effects of Laser Power. World Academy of Science, Engineering and Technology, 2017.

[17] Song X, Feih S, Zhai W, Sun CN, Li F, Maiti R, Wei J, Yang Y, Oancea V, Brandt LR, Korsunsky AM. Advances in Additive Manufacturing Process Simulation: Residual Stresses and Distortion Predictions in Complex Metallic Components. Materials & Design, 2020.

[18] Cattenone A, Morganti S, Alaimo G, Auricchio F. Finite element analysis of Additive Manufacturing based on Fused Deposition Modeling (FDM): distortion prediction and comparison with experimental data. Journal of Manufacturing Science and Engineering.

[19] Lachmayer L, Ekanayaka V, Hürkamp A, Raatz A. Approach to an optimized printing path for additive manufacturing in construction utilizing FEM modeling. 54th CIRP Conference on Manufacturing Systems, 2021.

[20] Alsoufi MS, El-sayed A. Warping Deformation of Desktop 3D Printed Parts Manufactured by Open Source Fused Deposition Modeling (FDM) System. International Journal of Mechanical & Mechatronics Engineering , 2017.

[21] Duty C, Failla J, Kim S, Lindahl J, Post B, Love L, Kunc V. Reducing mechanical anisotropy in extrusion-based printed parts. Proceedings of the 28th Annual International Solid Freeform Fabrication Symposium – An Additive Manufacturing Conference, 2017.

[22] Song D, Baek AMC, Koo J, Busogi M, Kim N. Forecasting Warping Deformation Using Multivariate Thermal Time Series and K-Nearest Neighbors in Fused Deposition Modeling. Applied Sciences, 2020.

[23] Federowicz K, Kaszynska M, Zielinski A, Hoffmann M. Effect of Curing Methods on Shrinkage Development in 3D-Printed Concrete. Materials, 2020.

[24] Li Z, Hojati M, Wu Z, Piasente J, Ashrafi N, Duarte JP, Nazarian S, Bilén SG, Memari AM, Radlinska A. Fresh and Hardened Properties of Extrusion-Based 3D-Printed Cementitious Materials: A Review. Sustainability, 2020.

[25] Suiker ASJ, Wolfs RJM, Lucas SM, Salet TAM. Elastic buckling and plastic collapse during 3D concrete printing. Cement and Concrete Research, 2020.

.